

Article

Controls on Nitrous Oxide Production in, and Fluxes from a Coastal Aquifer in Long Island, NY, USA

Caitlin Young ^{1,2,*}, Jonathan B. Martin ² and Gilbert N. Hanson ¹

¹ Geosciences Department, Stony Brook University, Stony Brook, NY 11794, USA; gilbert.hanson@stonybrook.edu

² Geosciences Department, University of Florida, Gainesville, FL 32611, USA; jbmartin@ufl.edu

* Correspondence: caitlin.young@ufl.edu; Tel: +1-631-415-7095

Academic Editor: Henry J. Bokuniewicz

Received: 27 June 2016; Accepted: 19 October 2016; Published: 4 November 2016

Abstract: Nitrous oxide (N₂O) has 265 times greater greenhouse potential than carbon dioxide and its atmospheric concentration has increased by about 20% since industrialization; however, N₂O production and emissions from aquatic systems are poorly constrained. To evaluate N₂O fluxes associated with meteoric groundwater discharge to coastal zones, we measured N₂O concentrations in May and October 2011 from two discharge points of the Upper Glacial aquifer on Long Island, NY, USA. One coastal zone contains only fresh water and the other contains an upper saline zone. N₂O concentrations decreased by around 40% for the fresh water and a factor of two for the salt water from May to October, 2011. Fluxes were around 100 to 200 times greater from the freshwater (246 to 448 μmol/m shoreline/day) than saltwater aquifer (26.1 to 26.5 μmol/m shoreline/day). N₂O concentrations correlate positively with NO₃⁻ and dissolved oxygen concentrations and negatively with salinity, dissolved organic carbon (DOC) and N₂ denitrification concentrations. The smaller saltwater N₂O export resulted from DOC enrichment in the upper saline zone, which appears to have driven denitrification to completion, removed N₂O, and increased N₂ denitrification. DOC concentrations should be considered in global N₂O flux estimates for coastal aquifers.

Keywords: nitrous oxide; coastal aquifer; submarine groundwater discharge; subterranean estuary; denitrification; Long Island Sound

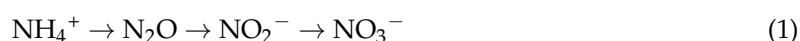
1. Introduction

Nitrous oxide (N₂O) is a powerful greenhouse gas with a greenhouse potential approximately 265 times that of CO₂ [1]. Atmospheric N₂O concentrations have increased from 270 ppb during pre-industrial times to the current value of around 327 ppb, and yet its global budget, particularly atmospheric fluxes from estuaries, rivers and groundwater, is still poorly understood. The increase in atmospheric N₂O concentrations largely results from anthropogenic activities that increase reactive N, including fixation of atmospheric N₂ through the Haber-Bosch process, increased cultivation of biological nitrogen fixers, such as legumes and rice, and burning of fossil fuels [2–4]. This rate of increase is accelerating; N₂O concentrations increased faster from 2013 to 2014 than average rates of increase during the preceding decade [5].

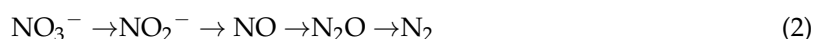
About two thirds of the uncertainty of the N₂O budget originates from limited information about N₂O emissions from agricultural leaching and runoff, human sewage, and atmospheric deposition, according to the Intergovernmental Panel on Climate Change (IPCC) 5th assessment report [6]. According to this methodology leaching and runoff comprises about half of the uncertainty in calculating the total agricultural source. Indirect N₂O sources are defined as the sum of N₂O lost from agricultural applications through gas volatilization (N₂O (G)), human consumption of crops followed by municipal sewage treatment (N₂O (S)), nitrogen leaching and runoff (N₂O (L)) [1]. Nitrogen

leaching (N_2O (L)) contributes ~75% of the indirect N_2O source and is derived from estuaries, rivers and groundwater [7]. The amount of N_2O lost from these settings is quantified by emission factors, termed EF5, which are calculated as the ratio of N_2O produced to the initial amount of inorganic nitrogen (NO_x and NH_4^+) in the system. Each of the three hydrologic pathways, which are referred to as EF5-e (estuaries), EF5-r (rivers), and EF5-g (groundwater) has an assigned EF5 value of 0.0025 by the IPCC 5th assessment report. Previous IPCC assessment reports had varying EF5 for each of the hydrologic pathways, due to uncertainty surrounding the calculation of emission factors. Uncertainty around the emission factors from estuaries, rivers, and groundwater stems from (1) small number of studies; (2) variability in study methodology and (3) differences in biogeochemical reactions within each setting.

N_2O production by biogeochemical reactions is well understood in terrestrial systems, but less so in coastal systems. In terrestrial systems experiments in which addition of five different N-bearing chemical fertilizers were correlated with N_2O emission in both aerobic and anaerobic agricultural and non-agricultural systems found denitrification of NO_3^- contributed the most to total N_2O emissions [8]. Coastal systems should also be an important for N_2O production because the interface between fresh and salt water is a biogeochemical hot spot [9–11] where N_2O forms as an intermediate product in both nitrification and denitrification processes. The oxidation of ammonium (NH_4^+) to nitrate yields N_2O as a byproduct of nitrification under aerobic conditions in soils and open water (1).



In hypoxic environments denitrification usually results in the formation of N_2 , a net sink of N from the environment, but can also terminate in N_2O (2) [12].



These reactions indicate that N_2O production in aquatic systems depends on the amount of total dissolved inorganic nitrogen (DIN; including NO_3^- , NO_2^- and NH_4^+) [13], as well as the oxidation states of mixed fresh groundwater and saline surface water in coastal aquifers [14,15]. Oxidation of NH_4^+ promotes N_2O production in mangrove sediments [16,17] and in estuarine water columns [18]. Denitrification of NO_3^- produces N_2O in intertidal sediments [19–21] which have low oxygen concentrations when they flood during high tide, and increased oxygen concentrations when exposed at low tide [22]. Intertidal fluxes of N_2O from muddy and sandy sediments are strongly correlated to NO_3^- availability and therefore extent of denitrification in the porewater [11,23].

Land use in the catchment area of coastal aquifers affects the amount of nitrogen available in porewater, which should in turn impact porewater N_2O concentrations. In Port Jefferson Harbor, a Long Island Sound embayment, land use in the coastal aquifer catchment area ranges from undeveloped to high density development. As a result, submarine groundwater discharge (SGD) derived nitrate loading varies by two orders of magnitude along the embayment coastline, with catchment areas containing high density development contributing more than 70% of the nitrate load to surface water [24]. In West Falmouth Harbor, MA the highest measured N_2O fluxes from the coastal aquifer were located in a nitrogen rich wastewater plume [11]. A summary of N_2O fluxes from temperate coastal sediments presented by Moseman-Valtierra et al., (2015) found average values range from $0.1 \mu\text{mol}\cdot\text{m}^{-2}\cdot\text{h}^{-1}$ to $10.1 \mu\text{mol}\cdot\text{m}^{-2}\cdot\text{h}^{-1}$, with the highest fluxes occurring when sediments received nitrogen amendments. These studies highlight the need for better understanding of how nitrogen additions to groundwater will impact N_2O fluxes to coastal waters, particularly as anthropogenic nitrogen degrades coastal waters worldwide [25].

In this paper, we describe intertidal sediment porewater N_2O concentrations from two discharge sites for a coastal aquifer on Long Island, NY, USA, which have similar sediment compositions. Each aquifer has distinct N_2O concentrations and distributions in time and space, which we interpret here in terms of the biogeochemical factors that control N_2O production. We calculated N_2O emission factors to place our measurements in a broader context and compared our values with those used

by the Intergovernmental Panel on Climate Change (IPCC) [7]. We describe how dissolved organic carbon (DOC) in porewater impacts N_2O concentrations and consequently N_2O flux to surface waters. This work provides a framework for how DOC and salinity can act as a proxy for N_2O concentrations in shallow porewater, which will help refine N_2O flux at the embayment and coastline scale.

2. Materials and Methods

2.1. Site Description

Porewater samples were collected from the Upper Glacial aquifer where it discharges to two embayments (Stony Brook Harbor, SBH and Port Jefferson Harbor, PJH) of Long Island Sound (Figure 1). The Upper Glacial aquifer consists of medium to coarse grain sands interbedded with clay lenses and contains elevated NO_3^- concentrations due to septic/sewage and lawn fertilizer loading [26]. The two field sites have different land use; Port Jefferson Harbor has medium to high density housing whereas in Stony Brook Harbor has low density housing or is forested [24]. These different land uses affect NO_3^- discharge via submarine groundwater discharge (SGD), with greater fluxes from more urbanized settings [24,27]. Both the fresh groundwater and saline coastal water endmembers are well oxygenated, limiting the extent of denitrification in the inland aquifer [28]. Both harbors have an ~2 m daily tidal range and undergo periodic dredging to maintain shipping channels [29]. Port Jefferson Harbor receives no fresh surface water, but undergoes tidal exchange with Long Island Sound and two small adjacent harbors; Conscience Bay and Setauket Harbor. The narrow (75 m) inlet of Stony Brook Harbor is bounded by West Meadow Creek, which provides limited amount of freshwater to the southern lobe of the harbor during high tide [29]. Inland topography at the Port Jefferson field site is steep. Consequently large hydraulic gradient between the groundwater and adjacent surface water drives freshwater towards the coast and prevents intrusion of saline coastal water during tidal inundation [27].

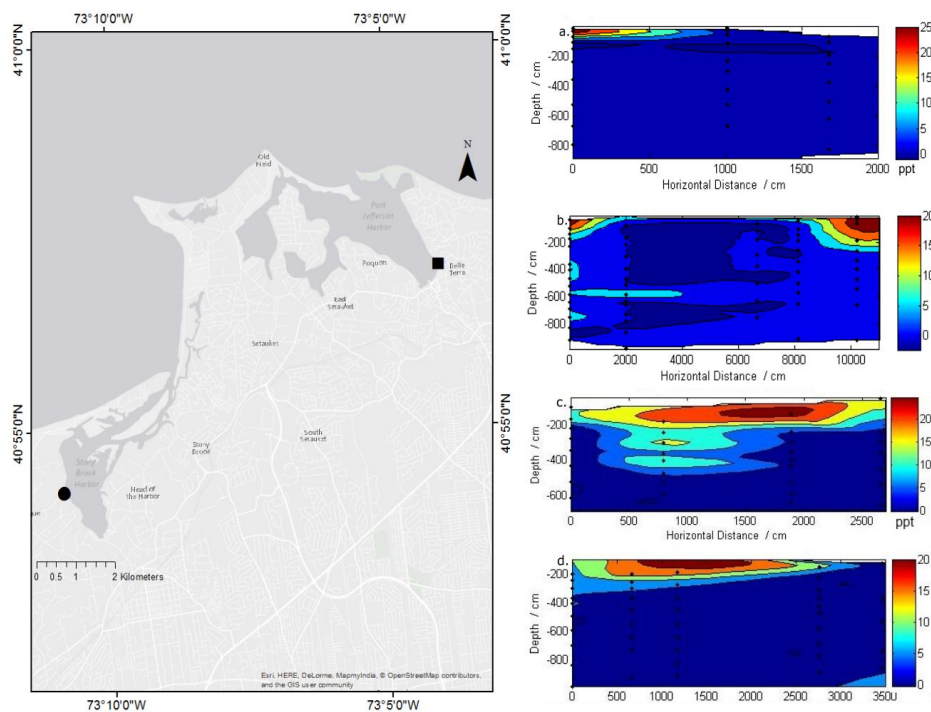


Figure 1. Site map of Port Jefferson Harbor coastal aquifer (■) and Stony Brook Harbor (SBH) coastal aquifer (●) located on embayment’s of Long Island Sound (left). Cross section of salinity at Port Jefferson Harbor during (a) May 2011 and (b) October 2011 and Stony Brook Harbor in (c) May 2011 and (d) October 2011. Sampling points (●) are shown for porewater samples at both sites (a–d).

2.2. Field Sampling and Observations

SGD rate measurements were taken using ultrasonic seepage meters in May and October 2011 and by manual seepage meter at each site in August 2012 [30]. Details of seepage meter results are presented elsewhere [31] and summarized below. Porewater was collected in May and October of 2011 simultaneous with the seepage meter sampling. These dates were chosen to minimize differences in porewater and atmospheric temperatures during sampling and to assess temporal variability in nitrous oxide dynamics. Porewater was sampled using an AMS Retract-A-Tip vapor probe [32] connected to a peristaltic pump with low gas permeability Viton tubing. Temperature, conductivity, pH, and dissolved oxygen were measured in the field by YSI 556 multi-parameter probe connected to an overflow cell. Nutrient samples were filtered (Whatman GF/B 0.45 μm), kept on ice while in the field, and frozen within 8 h of collection. Dissolved N_2/Ar samples were collected into 12 mL gastight vials (LabCo, Lampeter, UK), inverted and stored under deionized water at 4 $^\circ\text{C}$ until analysis. Dissolved N_2O samples were collected into pre-evacuated 9 mL vials (Grace-Discovery Sciences) with Teflon butyl septa crimp caps (MicroLiter Analytical, Suwanee, GA, USA). Samples were collected into glass syringes and loaded into vials with no headspace with the addition of 100 μL 0.1 M sodium azide to prevent microbial alteration of the sample. Field duplicates were collected for 10% of the total number of porewater sampling depths.

2.3. Laboratory Analyses

Nitrate (as $\text{NO}_3^- + \text{NO}_2^-$) concentrations were analyzed on a Lachat Quickchem auto-analyzer with a precision of $\pm 5\%$ for triplicate sample analysis. Dissolved organic carbon (DOC) was analyzed using a Shimadzu TC- total organic carbon analyzer. Dissolved N_2O concentrations were determined with gas chromatography following headspace extraction. Briefly, 3 mL of helium was injected into the headspace of sample vials, displacing 3 mL of sample. Samples were equilibrated at 25 $^\circ\text{C}$ for 2 h on a shaker table. Equilibrated headspace gas was analyzed on a gas chromatograph equipped with an electron capture device (Shimadzu GC-14a) at the Cary Ecosystems Institute. Replicates were analyzed for each sampling site and time period with a mean precision of $\pm 8\%$. Dissolved N_2/Ar concentrations were analyzed by membrane inlet mass spectrometry (MIMS) at the University of California, Davis [33]. Instrument drift was determined from analyses of deionized water held at a constant temperature (15 $^\circ\text{C}$) which was analyzed every 10–15 samples. Precision was 0.05 for N_2/Ar , calculated as the deviation of reference water from theoretical solubility values [34].

2.4. Calculation of Excess N_2 , Emission Factors (EF5), and N_2O Flux to Surface Waters

Solubility concentrations of N_2 and N_2O were calculated using equations of Weiss and Price [34,35]. For both gases, dissolved argon was used as an inert tracer to correct for physical effects of temperature, pressure and salinity [36]. Dissolved N_2O concentrations were calculated according to:

$$\text{N}_2\text{O}_{pw} = \frac{K_o x' P V_{wp} + \frac{x' P V_{hs}}{RT}}{V_{wp}} \quad (3)$$

where N_2O_{pw} is the concentration of N_2O in the porewater sample ($\text{nmol}\cdot\text{L}^{-1}$), K_o is the solubility coefficient for N_2O ($\text{mol}\cdot\text{L}^{-1}\cdot\text{atm}^{-1}$) derived from Weiss and Price (1980), x' is the dry gas mole fraction of N_2O in the sample headspace, P is the atmospheric pressure (1 atm), V_{wp} is the volume of the water phase (mL), V_{hs} is the volume of the headspace (mL), R is the gas constant ($\text{L}\cdot\text{atm}\cdot\text{K}^{-1}\cdot\text{mol}^{-1}$) and T is the temperature (K) [35,37].

The total concentration of dissolved N₂ in a sample is equal to

$$N_{2 \text{ denitrification}} = N_{2 \text{ total}} - (N_{2 \text{ atm. eq}} + N_{2 \text{ EA}}) \quad (4)$$

where N_{2 total} is the total concentration of N₂ in the sample, N_{2 atm. eq} is the amount of N₂ present due to solubility dependent atmospheric equilibration [34] corrected for salinity and recharge temperature, N_{2 EA} is the amount of N₂ due to excess air entrainment and N_{2 denitrification} is the remaining amount of N₂ in the sample, which is assumed to result from denitrification. Excess air entrainment occurs when bubbles trapped at the capillary fringe dissolve, either partially or completely, into groundwater during recharge [38]. During complete bubble dissolution the amount of excess air in the sample will have N₂/Ar ratios representative of atmospheric molar ratios whereas during incomplete bubble dissolution N₂/Ar ratios will be lower than atmospheric ratios as Ar solubility is greater than N₂ solubility [39]. As bubble dissolution approaches completion this lower value will be close to the N₂/Ar ratio for air-equilibrated water at the recharge temperature [40]. As we are unable to determine the extent of bubble dissolution for a given groundwater recharge scenario, we calculate the minimum and maximum amount of excess air and use the average of these to values to calculate the amount of N₂ denitrification in each sample.

$$N_{2 \text{ EA max}} = X_{\text{Ar T}} - X_{\text{Ar Eq}} \times (X_{\text{N2 atm}}/X_{\text{Ar atm}}) \quad (5)$$

$$N_{2 \text{ EA min}} = X_{\text{Ar T}} - X_{\text{Ar Eq}} \times (X_{\text{N2 EQ}}/X_{\text{Ar EQ}}) \quad (6)$$

where N_{2 EA max} and N_{2 EA min} are the maximum and minimum excess air incorporations, X_{Ar T} is the concentration of dissolved argon in the sample and X_{Ar Eq} is the argon concentration in equilibrium with the atmosphere. X_{N2 atm} and X_{Ar atm} are the mole fractions of N₂ and Ar in the atmosphere respectively, reflecting complete dissolution, and X_{N2 EQ} and X_{Ar EQ} are the equilibrium mole fractions of N₂ and Ar respectively. We use Equations (5) and (6) to calculate the lower and upper values for N_{2 EA} in porewater and use the mean N_{2 EA} to determine the best estimate of N_{2 denitrification} according to Equation (2).

If NO₃⁻ is denitrified prior to discharged, then dissolved N₂ and N₂O gas concentrations may indicate the initial nitrate concentration by:

$$\text{NO}_3^- \text{ initial} = \text{NO}_3^- \text{ final} + N_{2 \text{ denitrification}} + N_2\text{O} \quad (7)$$

Considering the sequence of denitrification (2) where the NO₃⁻ initial (μmol·L⁻¹) is the initial nitrate concentration, NO₃⁻ final (μmol·L⁻¹) is the concentration of nitrate in the porewater sample, N₂O (μmol·L⁻¹) is the concentration of dissolved N₂O and N_{2 denitrification} is the amount of N₂ attributable to denitrification in the porewater sample. Here we used initial nitrate concentration to calculate EF for two coastal aquifers (EF5):

$$\text{EF5} = \frac{N_2\text{O}}{\text{NO}_3^- \text{ initial}} \quad (8)$$

where N₂O is the concentration of N₂O in a sample and NO₃⁻ initial is as defined in Equation (7).

Fluxes of N₂O to surface water were calculated by multiplying the N₂O concentration from the shoreward-most porewater concentrations by the SGD rate for the given sample location and time period. The shoreward most porewater profile lies within the zone of low tide discharge, where seepage meters were placed to measure SGD rates (cm·d⁻¹). The N₂O concentration was taken from the shallowest sampling point, typically <50 cm below the sediment water interface, to estimate N₂O fluxes.

2.5. Statistical Analysis

Multivariate and correlation analysis was performed using JMP 10. Two factor ANOVA analyses were used to test for differences in N_2O concentrations between site (factor 1) and date (factor 2). Samples were pooled according to site and sampling period (May and October). Sample collection required a period of 4 consecutive days for each individual site and date. Therefore, tide stage was not considered in the ANOVA analysis. Sample variability, as determined from field duplicates, was less than 8% for the statistical parameters examined by ANOVA and PCA. Principal component analysis (PCA) was used to compare primary variables (salinity, dissolved oxygen, NO_3^- , N_2O , DOC, and N_2 denitrification, and distance offshore) in these two coastal aquifers to assess which may relate to N_2O production.

3. Results

Seepage rates were consistent across each sampling time (May 2011, October 2011 and August 2012) in each of the different sites. Seepage rates ranged from $76 \text{ cm}\cdot\text{day}^{-1}$ to $149 \text{ cm}\cdot\text{day}^{-1}$ [31] in Port Jefferson Harbor and from 26 to $102 \text{ cm}\cdot\text{day}^{-1}$ in Stony Brook Harbor.

3.1. Spatial Distribution of Solutes and N_2O Concentrations

In PJH the coastal aquifer was largely fresh in both May and October (Figure 1) with salinity below ~ 2 for all samples except for a shallow sample with a salinity of 16.3 from the high tide rack line at a depth of 66 cm (Figure 1). The elevated salinity suggests saltwater is not flushed as rapidly in this zone. SBH exhibits an upper saline zone in which the salinity ranges from 3.9 to 17.8. Below the upper salinity zone, the salinity is < 2 . In May saline water in the upper saline zone (USZ) penetrated to a depth of ~ 3 m but in October it only penetrated to a depth of ~ 2 m. N_2O concentrations differed between the two harbors and sampling dates (Figure 2). Porewater at PJH had N_2O concentrations ranging $78 \text{ nmol}\cdot\text{L}^{-1}$ to $399 \text{ nmol}\cdot\text{L}^{-1}$ (average $97 \pm 91 \text{ nmol}\cdot\text{L}^{-1}$) in May and $46 \text{ nmol}\cdot\text{L}^{-1}$ to $267 \text{ nmol}\cdot\text{L}^{-1}$ in October (average $141 \pm 77 \text{ nmol}\cdot\text{L}^{-1}$) (Figure 3a). Porewater at SBH had N_2O concentrations ranged $0 \text{ nmol}\cdot\text{L}^{-1}$ to $719 \text{ nmol}\cdot\text{L}^{-1}$ (average $218 \pm 197 \text{ nmol}\cdot\text{L}^{-1}$) in May and $0 \text{ nmol}\cdot\text{L}^{-1}$ to $493 \text{ nmol}\cdot\text{L}^{-1}$ (average $101 \pm 93 \text{ nmol}\cdot\text{L}^{-1}$) in October. Dissolved organic carbon (DOC) concentrations in porewater from PJH averaged $28.7 \pm 9.9 \text{ }\mu\text{mol}\cdot\text{L}^{-1}$ and $37.5 \pm 30.5 \text{ }\mu\text{mol}\cdot\text{L}^{-1}$ in May and October respectively, lower than the average SBH porewater DOC concentrations, which were $175.9 \pm 82.0 \text{ }\mu\text{mol}\cdot\text{L}^{-1}$ and $146.5 \pm 249.7 \text{ }\mu\text{mol}\cdot\text{L}^{-1}$ in May and October respectively. At SBH a single outlier contained DOC concentration of $1253.6 \text{ }\mu\text{mol}\cdot\text{L}^{-1}$. Porewater NO_3^- concentrations at PJH averaged $281.6 \pm 94.1 \text{ }\mu\text{mol}\cdot\text{L}^{-1}$ and $168.1 \pm 73.4 \text{ }\mu\text{mol}\cdot\text{L}^{-1}$ in May and October respectively, and were similar at SBH, with average concentrations of $187.2 \pm 113.2 \text{ }\mu\text{mol}\cdot\text{L}^{-1}$ in May and $315.6 \pm 24.6 \text{ }\mu\text{mol}\cdot\text{L}^{-1}$ in October (Figure 3c). Dissolved oxygen saturation at PJH averaged 52.8% in May and 58.4% in October and was similar, but with a wider range, at SBH with values of 70.8% in May and 56.6% in October (Figure 3d). Excess N_2 was not detected in all samples, with average concentrations at PJH of $42 \pm 37 \text{ }\mu\text{mol}\cdot\text{L}^{-1}$ in May and 58.4 ± 8.4 in October, with similar values at SBH with average concentrations of $58.3 \pm 57 \text{ }\mu\text{mol}\cdot\text{L}^{-1}$ in May and $30.8 \pm 57 \text{ }\mu\text{mol}\cdot\text{L}^{-1}$ in October (Figure 3e).

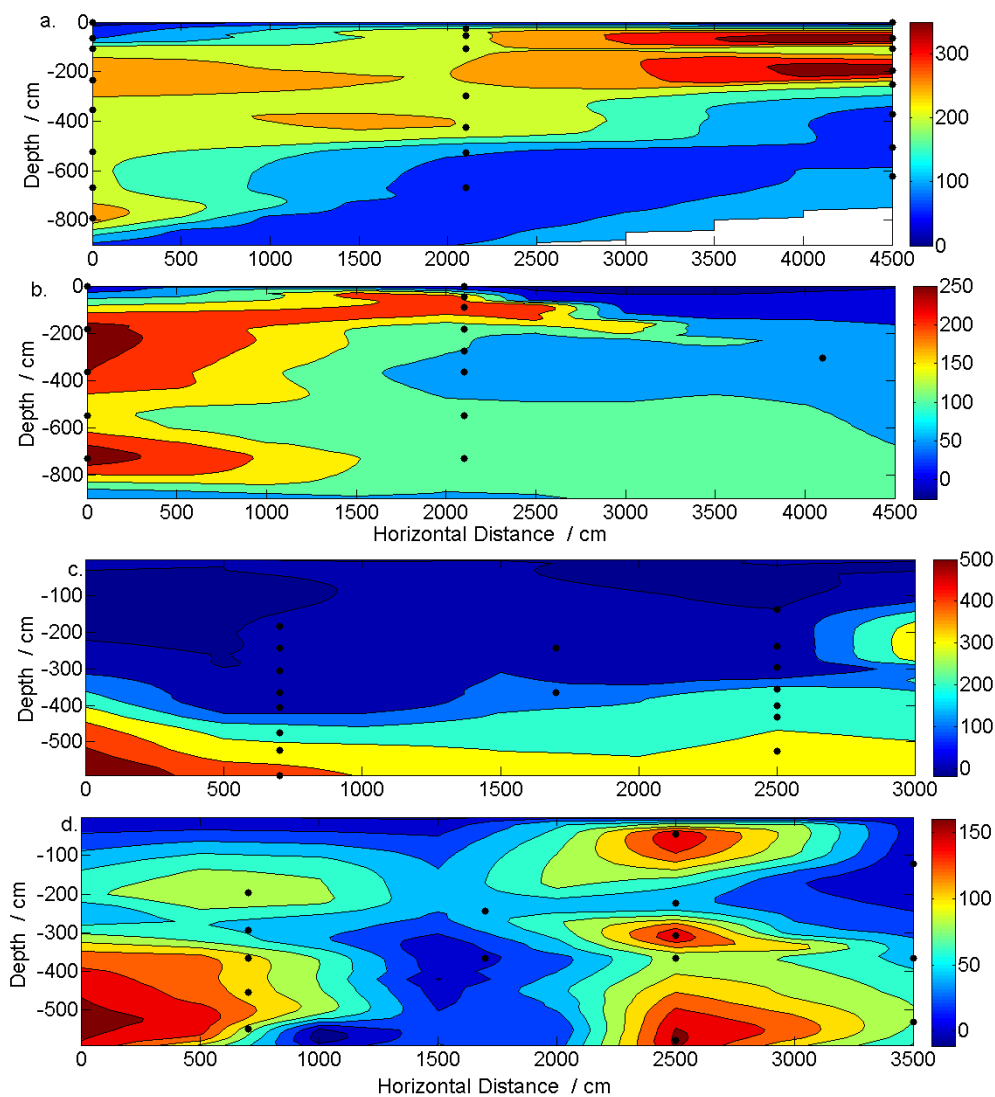


Figure 2. Cross section of Nitrous oxide (N_2O) concentrations ($\text{nmol}\cdot\text{L}^{-1}$) for Port Jefferson Harbor in (a) May and (b) October and Stony Brook Harbor in (c) May and (d) October. Black dots (●) indicate individual porewater sampling points.

Lumped N_2O concentrations from both sites were not normally distributed, but were skewed due to a high number of zero values at SBH. ANOVA tests show statistically different N_2O concentrations ($p < 0.002$), salinity ($p < 0.032$) and DOC concentrations ($p < 0.015$) between PJH and SBH but not between sampling periods at individual sites. Data were broken down by site to test for differences between sampling periods. ANOVA tests show statistically different N_2 denitrification ($p < 0.001$), and temperature ($p < 0.0001$) between the May and October sampling periods at each location. Data from both sites during May and October show a positive correlation between salinity and DOC concentration ($r^2 = 0.58$, $p < 0.0001$) (Figure A1). NO_3^- concentration is negatively correlated with salinity ($r^2 = 0.48$, $p < 0.021$) (Figure A2) in SBH porewater from May, but NO_3^- is otherwise not correlated with salinity. DOC concentration is positively correlated with N_2 denitrification ($p = 0.0069$) at both sites. NO_3^- concentrations and dissolved oxygen concentrations were not statistically different between sites or sampling time period.

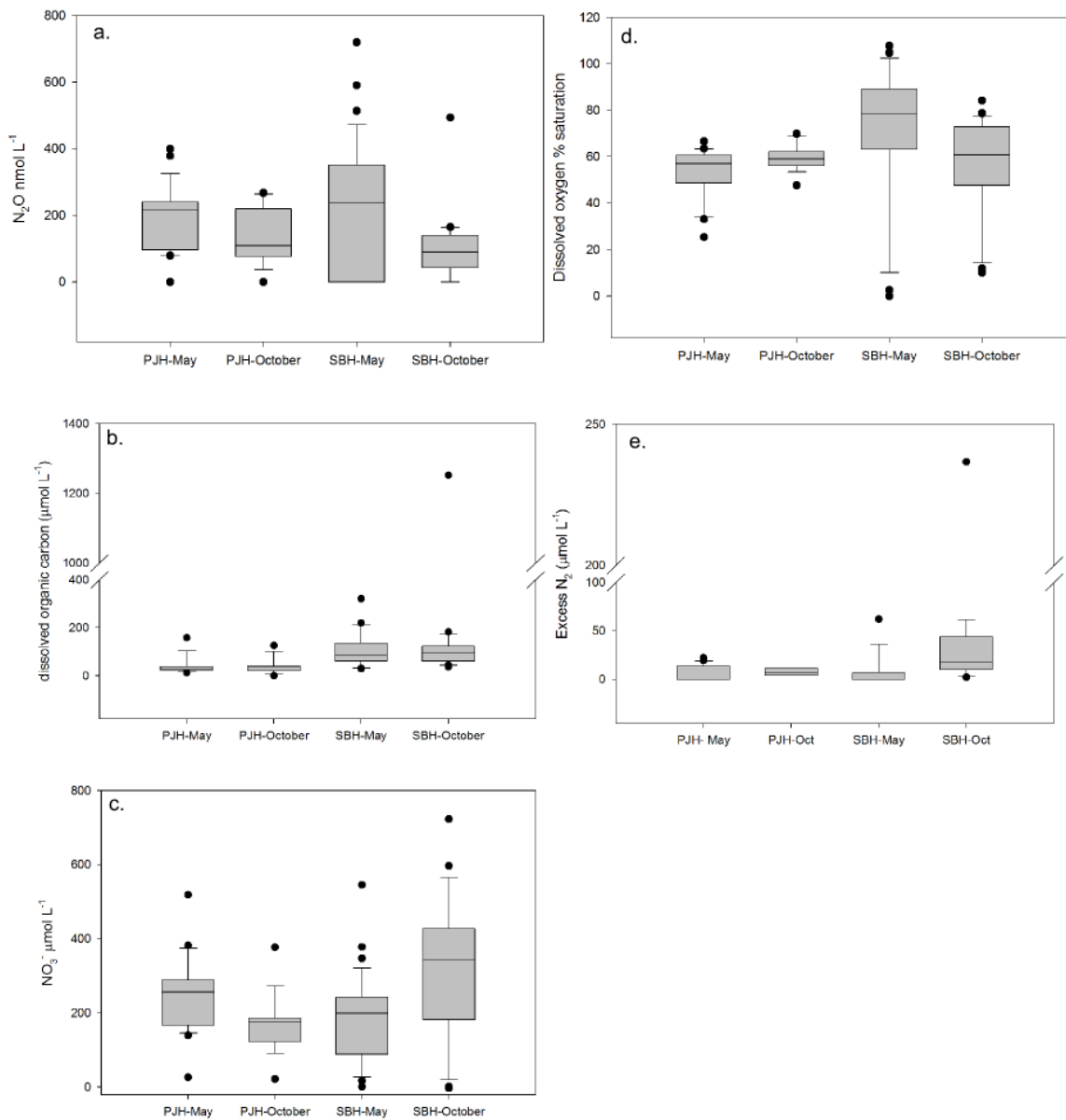


Figure 3. Box-and-whisker plots of (a) N_2O concentrations; (b) dissolved organic carbon concentrations; (c) NO_3^- concentrations; (d) dissolved oxygen % saturation and (e) N_2 denitrification concentrations for SBH and PJH porewater in May and October.

A principal component analysis (PCA) was performed individually for PJH and SBH. At each site data from both sampling time periods was merged to provide a data set sufficiently large for the analyses. At PJH the first component explains 44% of the variation and the second component explains 20.3% of the variation (Figure 4a). At PJH N_2O and NO_3^- concentrations plot closely together and are at 180° from N_2 denitrification but are $\sim 90^\circ$ from DO% and DOC concentrations. The SBH PCA found the first component explains 45% of the variation and the second component explains 17% of the variation (Figure 4b). Variables N_2O concentration, NO_3^- concentration and DO% plot close together but are at 180° from salinity and DOC concentration.

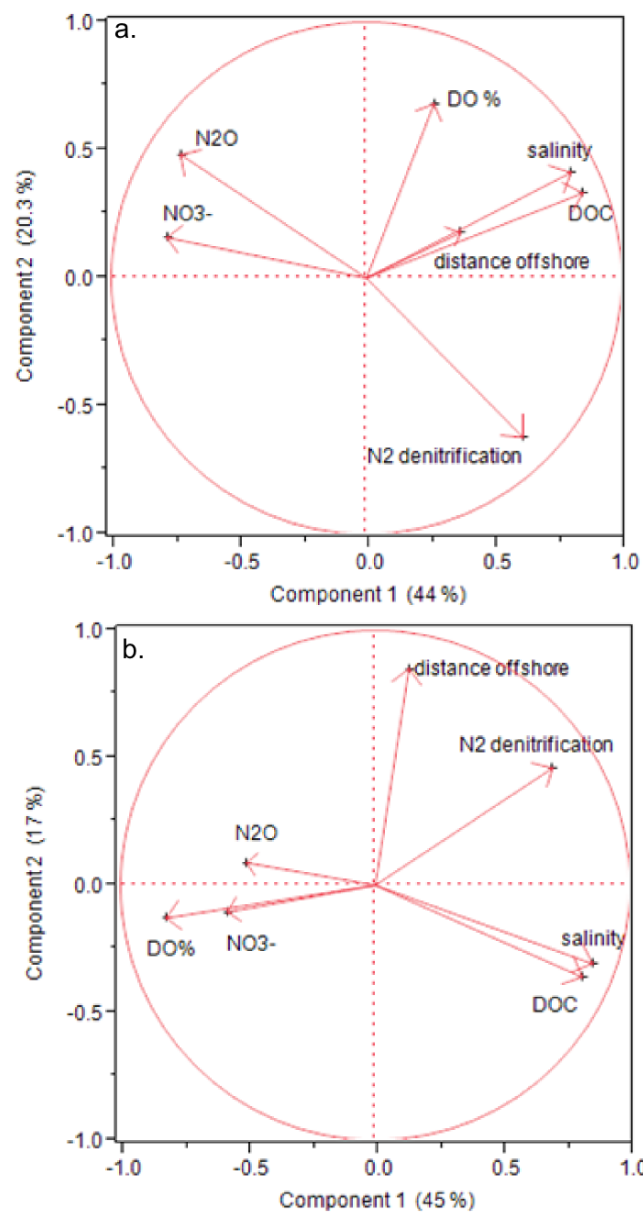


Figure 4. Principal component analysis (PCA) of the major nitrogen cycling geochemical solutes in porewater from (a) Port Jefferson Harbor and (b) Stony Brook Harbor.

3.2. Flux of N₂O to Surface Waters

Multiplying the measured SGD rates by the subtidal shallow N₂O concentration yields an average N₂O flux from PJH of 448 μmol/m shoreline/d and 246 μmol/m shoreline/d for May and October sampling respectively (Figure 5). At the discharge point shoreward of the upper saline zone at SBH N₂O flux averaged 26.5 μmol/m shoreline/d and 26.1 μmol/m shoreline/d for May and October respectively (Figure 5). Errors were calculated based on the range of measured SGD rates recorded at the two sites during sampling times in May and October of 2011. Error bars encompass the standard deviation for SGD measurements for each site and thus give an overall range of N₂O fluxes calculated for each site and sampling date. Only the shallowest N₂O concentration was used for each site and sampling date.

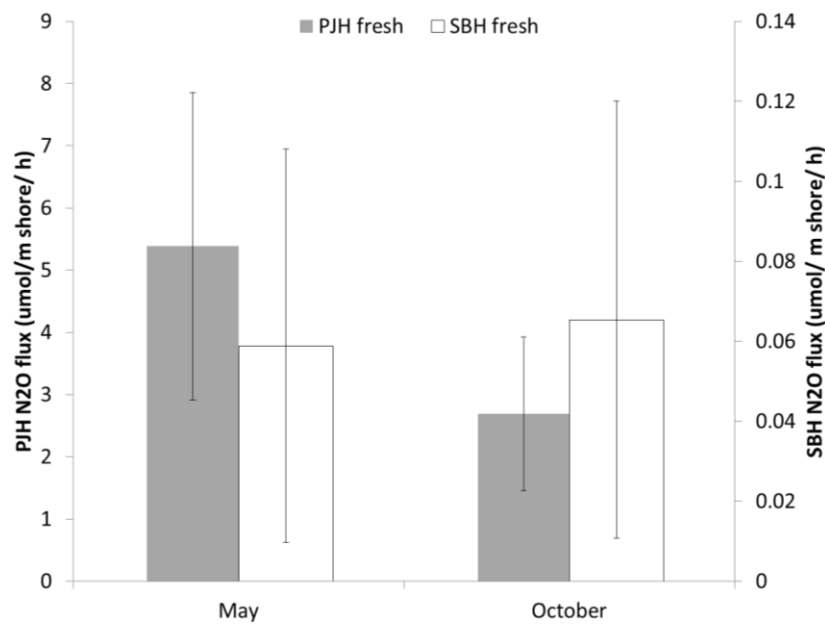


Figure 5. N₂O flux from a fresh coastal aquifer (PJH) and a coastal aquifer containing an USZ (SBH). Error bars are calculated from the range of submarine groundwater discharge (SGD) flux measurements taken for each site during the respective time periods.

3.3. Emission Factor (EF5)

Emission factors (Equation (8)) were calculated for each site, inclusive of all porewater samples for each sampling period. Average EF5 values for PJH were 4.2×10^{-3} and 8.0×10^{-4} in May and October respectively. Average EF5 values for SBH were 9.0×10^{-4} and 6.0×10^{-4} in May and October respectively (Table 1).

Table 1. Emission factors (EF5). Mean and median calculated from all porewater samples at each coastal aquifer.

Month	PJH		SBH	
	Mean	Median	Mean	Median
May	0.0042	0.0008	0.0009	0.0011
October	0.0008	0.0008	0.0006	0.0002

4. Discussion

4.1. N₂O in Fresh and Saline Coastal Aquifers

Salinity distributions of coastal aquifers depend on the balance between inland hydraulic head and elevation of adjacent coastal water bodies [41,42]. This balance affects salinity distribution at SBH and PJH. An upper saline zone (USZ) forms at SBH because of the tides and waves [42–44], but the USZ is missing at PJH because SGD rates are greater there than SBH because of higher inland elevations (Figure 1) [27]. DOC concentrations are greater than in Long Island Sound surface water than in the pore water in the upper Glacial aquifer [28]. Therefore, the correlation between porewater salinity and DOC concentration (Figure A1) suggests much DOC originates from mixing of surface estuarine water into the USZ. Elevated DOC concentrations of Long Island Sound reflect primary production in the photic zone and DOC remineralization in the pore water by elevated oxygen concentrations [45]. Circulation of saline surface water into shallow sediments at SBH thus provides a source of electron donors for reduction of inorganic nitrogen.

Although positive correlations have been found between N_2O fluxes and groundwater NO_3^- concentration in West Falmouth Harbor, Massachusetts, USA [11], in our study only porewater at SBH in May exhibits a positive correlation between NO_3^- concentrations and N_2O concentrations (Figure A2). Therefore, at these sites, groundwater NO_3^- concentration does not necessarily predict N_2O concentration, unlike West Falmouth Harbor [11]. The relationship between all the variables can be gleaned from PCA results. At PJH, PCA results indicate that NO_3^- and N_2O are positively correlated and are both inversely correlated with N_2 denitrification. Salinity, DOC, DO% and distance offshore (below mean high tide) are positively correlated with each other but are orthogonal to N_2O , NO_3^- and N_2 denitrification, indicating little correlation between these factors. The close relation between salinity, DOC, distance offshore and DO% reflects a saline water source of DOC and that saltwater intrusion depends on the distance offshore below mean high tide at PJH. NO_3^- and N_2O reduction produces N_2 denitrification (Equation (2)) resulting in their inverse correlation (Figure 4a). At SBH, salinity and DOC are closely linked because of the USZ, which is missing at PJH (Figure 1). A strong inverse relationship between DOC and N_2O indicates DOC drives the reduction of N_2O . The reduction of N_2O should result in the formation of N_2 denitrification, although this is not evident in the PCA analysis as N_2O and N_2 denitrification are orthogonal to each other.

In both PJH and SBH the third principal component explains 12%–14% of the variability and depends primarily on NO_3^- concentrations which suggests the porewater NO_3^- is independent of the other coastal aquifer parameters. Anthropogenic NO_3^- comprises the bulk of DIN inputs to the coastal aquifer system [46], therefore NO_3^- concentrations are dictated more by inputs to the upper Glacial aquifer than processes in the coastal zone. Given the overall low concentrations of N_2 denitrification and N_2O , when compared to other groundwater investigations in temperate sediments [11,47–49] it is evident that much of the groundwater NO_3^- is not denitrified during transit through the coastal aquifer.

Previous investigations in coastal aquifers do not consider DOC as a driver of N_2O reduction of an influence on N_2O flux to surface water. However, DOC is considered in determining N_2O concentrations of other settings, such as river and estuarine sediments. In a study of river sediments, N_2O production resulted from only 0.01% of the nitrate reduction when sediments were amended with carbon [50], and 6% of NO_3^- reduced formed NO_2^- with the balance of NO_3^- reduction continuing to form N_2 or NH_4^+ . Similar to these river settings, we find N_2O production to be negatively correlated with DOC concentration at SBH, where DOC is entrained in the aquifer in the USZ (Figure 4). Concentrations of N_2 denitrification were statistically different between PJH and SBH, with SBH having a higher mean N_2 denitrification concentration (Figure 3e). Therefore, the elevated DOC concentrations in the USZ of SBH appear to drive the reduction of N_2O to completion, resulting in an accumulation of N_2 and lower N_2O concentrations.

The recognition of a DOC-rich USZ as a sink for N_2O is critical in accurately predicting N_2O production in sandy coastal sediments. Benthic sediments consume N_2O , particularly in the presence of benthic algae cover [51]. In coastal sediments a lack of an USZ can occur due to a lack of tides or waves [52] or high freshwater hydraulic head. Where an USZ delivers carbon to the subterranean estuary, its remineralization will deplete pore water in DO and cause complete denitrification, removing N_2O from porewater. Understanding the salinity configuration, and thus the DOC concentrations, of sandy coastal aquifers will be important to estimating global N_2O concentrations and atmospheric fluxes from coastal sediments.

4.2. Temporal Variation in N_2O Production

N_2O concentrations vary temporally in groundwater [53], vadose zone [54] and coastal wetlands [47], and single time point sampling can lead to inaccuracies in mean annual N_2O flux to the atmosphere. At SBH and PJH average N_2O concentrations were greater in May than in October, despite no statistical difference in NO_3^- concentrations. The location of the maximum concentration changed between sample times; at PJH, maximum N_2O concentrations occurred in the shoreward-most

porewater at depths less than 2 m in May while maximum N₂O concentrations occurred near high tide at depths greater than 2 m in October (Figure 2a,b). At SBH, maximum N₂O concentrations occurred in the landward portion of the freshwater zone, at depths greater than 3 m in May, but in October maximum N₂O concentrations occurred at shoreward depths greater than 3 m and at shallow depths less than 1 m (Figure 2c,d).

The cause of these shifts in location of elevated N₂O concentrations through time likely relates to hydrological and biogeochemical reactions. Temporal variations in coastal aquifer heads can drive the saltwater-freshwater interface landward during winter months and seaward during the summer months (46), with additional freshwater recharge to catchment areas of subterranean estuaries due to recharge as snowmelt (49) or precipitation (50) increases water table height (48). Consequently, variations in freshwater discharge, with its elevated NO₃ concentrations, alter the overall composition of SGD (48) as the fresh fraction of SGD increases during spring and summer. Elevated NO₃ concentrations would limit complete denitrification and increase porewater N₂O concentrations, generating greater N₂O flux in the spring. This variation may help explain the subtidal maximum N₂O values observed in PJH (Figure 2). Causes are less clear for temporal variation in N₂O distribution in SBH. The absence of N₂O in shallow (<3 m) porewater in May is clearly linked to the presence of a DOC rich USZ, but the USZ does not reach depths greater than 2 m in October, possibly due to changes in wave or wind action, which have temporal patterns.

4.3. N₂O Flux Estimates and EF5

A review of 56 studies of N₂O fluxes from estuarine sediments found fluxes to range from -2.9 to 25.2 μmol·m⁻²·h⁻¹ from intertidal sediments, with an estimated global intertidal N₂O flux estimate of 0.007 to 0.05 Tg N₂O-N·year⁻¹ [13]. These values are low compared to global estimates of N₂O flux from estuarine open water, but are similar to estimates from mangroves and salt marshes. We estimate average N₂O fluxes to range from 0.06 to 0.07 μmol/m shoreline/h at SBH, which are the low end of fluxes observed from intertidal sediments (Figure 5). Our estimated fluxes are around two orders of magnitude greater at PJH than SBH, with average values ranging between 2.7 and m (Figure 5). In addition to the different DOC concentrations of the two aquifers and its control on the N₂O concentrations, the difference in fluxes between our two sites results from the large range in SGD rates from the two sites. The large range in flux values at two nearby sites points out the difficulty in establishing global N₂O fluxes from coastal aquifers and the strong need to distinguish the range in types of coastal aquifers and their control on SGD, which is poorly constrained (e.g., [55]).

The average EF5 values for all porewater sampled in PJH and SBH were 0.002 and 0.0007 respectively. The average value for PJH is similar to the value of 0.0025 used by the IPCC for groundwater, estuaries and rivers [3], but the EF5 for SBH is about 70% lower. The flux of N₂O from groundwater to the atmosphere is thought to be altered by transformations that occur in the overlying soil, such as nitrification [56]. Direct diffusive flux from aquifers to the atmosphere appears to be highly variable and depend on aquifer composition [57]. Our calculated EF5 values are an average of all porewater N₂O concentrations at each site and therefore differences in N₂O flux, driven by DOC inputs at SBH, are masked by the high N₂O concentrations in the freshwater portion of the aquifer. In addition, mean EF5 values at PJH are like those measured for groundwater and thus it is possible that the mixing of oxygenated seawater with oxygenated groundwater does not set up a sufficient geochemical gradient to alter the N₂O concentrations in the aquifer, which are derived from the groundwater endmember.

5. Conclusions

Production of N₂O in the coastal aquifers of PJH and SBH was regulated by high concentrations of NO₃⁻, but N₂O concentrations in shallow porewater were altered in the presence or absence of a DOC rich USZ. At SBH, the USZ was present due to tidal circulation of saline surface water. Saline surface water carries DOC which fuels denitrification resulting in a larger portion of NO₃⁻ reduced to

excess N_2 as opposed to N_2O . At PJH a large hydraulic gradient between groundwater and surface water prevented the formation of an upper saline zone, which limited the introduction of DOC and elevated the N_2O concentrations in shallow porewater. Average EF5 values for intertidal sediments of the coastal aquifers studied here are similar to those reported in the IPCC for estuaries, groundwater and rivers. An increase in anthropogenic nitrogen loading to coastal aquifers is likely to increase the total N_2O production in the groundwater endmember of coastal aquifers, ostensibly increasing N_2O flux to the atmosphere. Our data suggest processes such as sea level rise, which shallow the hydraulic gradient and result in the formation of upper saline zones in coastal aquifers, may offset some N_2O flux to the atmosphere as DOC inputs drive denitrification processes to completion, thereby removing N_2O from porewater prior to SGD.

Acknowledgments: This work was funded by New York SeaGrant (R-CTP-44-NYCT). Additional funding was provided to C.Y. SeaGrant Scholar Thesis Completion Award and by NSF grant OCE-1325227. Thank you to P. Groffman and the Cary Ecosystems Institute for N_2O analysis facilities.

Author Contributions: C.Y. and G.H. conceived and designed the investigation. C.Y. performed all fieldwork and sample analysis for the project. C.Y. analyzed the data. C.Y. wrote the manuscript. J.B.M. contributed intellectual ideas for data synthesis and manuscript preparation.

Conflicts of Interest: The authors declare no conflict of interest.

Appendix A

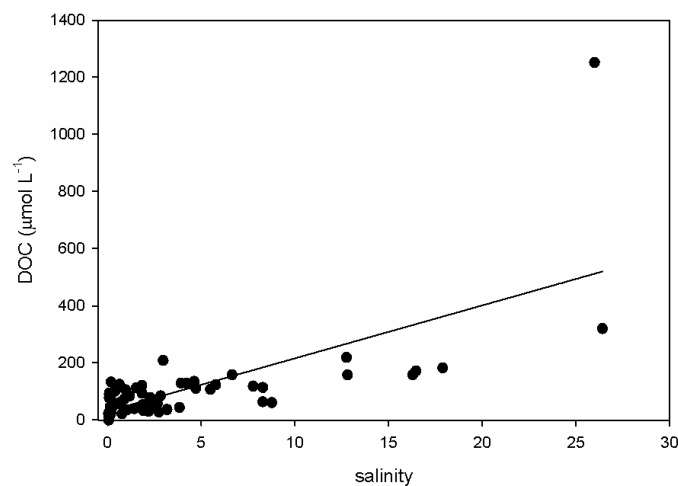


Figure A1. Cross plot of salinity vs. DOC concentration in all samples from SBH and PJH in 2011.

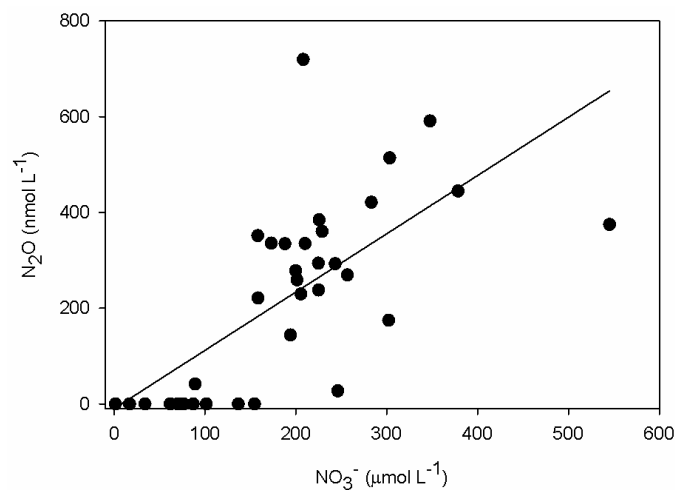


Figure A2. Cross plot of salinity vs. NO_3^- concentration in May 2011 porewater samples from SBH.

References

1. Forster, P.; Ramaswamy, V.; Artaxo, P.; Berntsen, T.; Betts, R.; Fahey, D.W.; Haywood, J.; Lean, J.; Lowe, D.C.; Myhre, G.; et al. *Changes in Atmospheric Constituents and in Radiative Forcing*; Cambridge University Press: Cambridge, UK, 2007.
2. Galloway, J.N.; Aber, J.D.; Erisman, J.W.; Seitzinger, S.P.; Howarth, R.W.; Cowling, E.B.; Cosby, B.J. The nitrogen cascade. *Bioscience* **2003**, *53*, 341–356. [[CrossRef](#)]
3. Denman, K.L.; Brasseur, G.; Chidthaisong, A.; Ciais, P.; Cox, P.M.; Dickinson, R.E.; Hauglustaine, D.; Heinze, C.; Holland, E.; Jacob, D.; et al. Couplings between changes in the climate system and biogeochemistry. In *Climate Change 2007: The Physical Science Basis. Contribution of Working Group I to the Fourth Assessment Report of the Intergovernmental Panel on Climate Change*; Solomon, S., Qin, D., Manning, M., Chen, Z., Marquis, M., Averyt, K.B., Tignor, M., Miller, H.L., Eds.; Cambridge University Press: Cambridge, UK; New York, NY, USA, 2007.
4. Erisman, J.W.; Sutton, M.A.; Galloway, J.; Klimont, Z.; Winiwarter, W. How a century of ammonia synthesis changed the world. *Nat. Geosci.* **2008**, *1*, 636–639. [[CrossRef](#)]
5. Davidson, E.A. The contribution of manure and fertilizer nitrogen to atmospheric nitrous oxide since 1860. *Nat. Geosci.* **2009**, *2*, 659–662. [[CrossRef](#)]
6. Nevison, C. Review of the IPCC methodology for estimating nitrous oxide emissions associated with agricultural leaching and runoff. *Chemosphere Glob. Chang. Sci.* **2000**, *2*, 493–500. [[CrossRef](#)]
7. IPCC. *Climate Change 2013: The Physical Science Basis. Contribution of Working Group I to the Fifth Assessment Report of the Intergovernmental Panel on Climate Change*; Stocker, T.F., Qin, D., Plattner, G.-K., Tignor, M., Allen, S.K., Boschung, J., Nauels, A., Xia, Y., Bex, V., Midgley, P.M., Eds.; Cambridge University Press: Cambridge, UK; New York, NY, USA, 2013.
8. Liu, L.; Greaver, T.L. A review of nitrogen enrichment effects on three biogenic GHGs: The CO₂ sink may be largely offset by stimulated N₂O and CH₄ emission. *Ecol. Lett.* **2009**, *12*, 1103–1117. [[CrossRef](#)] [[PubMed](#)]
9. Kroeger, K.D.; Charette, M.A. Nitrogen biogeochemistry of submarine groundwater discharge. *Limnol. Oceanogr.* **2008**, *53*, 1025–1039. [[CrossRef](#)]
10. Roy, M.; Martin, J.B.; Cherrier, J.; Cable, J.E.; Smith, C.G. Influence of sea level rise on iron diagenesis in an east Florida subterranean estuary. *Geochim. Cosmochim. Acta* **2010**, *74*, 5560–5573. [[CrossRef](#)]
11. Moseman-Valtierra, S.; Kroeger, K.D.; Crusius, J.; Baldwin, S.; Green, A.; Brooks, T.W.; Pugh, E. Substantial nitrous oxide emissions from intertidal sediments and groundwater in anthropogenically-impacted West Falmouth Harbor, Massachusetts. *Chemosphere* **2015**, *119*, 1281–1288. [[CrossRef](#)] [[PubMed](#)]
12. Ward, B.B. Nitrification in marine systems. In *Nitrogen in the Marine Environment*, 2nd ed.; Elsevier Academic Press Inc.: San Diego, CA, USA, 2008; pp. 199–261.
13. Murray, R.H.; Erler, D.V.; Eyre, B.D. Nitrous oxide fluxes in estuarine environments: Response to global change. *Glob. Chang. Biol.* **2015**, *21*, 3219–3245. [[CrossRef](#)] [[PubMed](#)]
14. Slomp, C.P.; van Cappellen, P. Nutrient inputs to the coastal ocean through submarine groundwater discharge: Controls and potential impact. *J. Hydrol.* **2004**, *295*, 64–86. [[CrossRef](#)]
15. Bratton, J.F. The three scales of submarine groundwater flow and discharge across passive continental margins. *J. Geol.* **2010**, *118*, 565–575. [[CrossRef](#)]
16. Corredor, J.E.; Morell, J.M.; Bauza, J. Atmospheric nitrous oxide fluxes from mangrove sediments. *Mar. Pollut. Bull.* **1999**, *38*, 473–478. [[CrossRef](#)]
17. Munoz-Hincapie, M.; Morell, J.M.; Corredor, J.E. Increase of nitrous oxide flux to the atmosphere upon nitrogen addition to red mangroves sediments. *Mar. Pollut. Bull.* **2002**, *44*, 992–996. [[CrossRef](#)]
18. Barnes, J.; Upstill-Goddard, R.C. N₂O seasonal distributions and air-sea exchange in UK estuaries: Implications for the tropospheric N₂O source from European coastal waters. *J. Geophys. Res. Biogeosci.* **2011**, *116*. [[CrossRef](#)]
19. Robinson, A.D.; Nedwell, D.B.; Harrison, R.M.; Ogilvie, B.G. Hypernutrified estuaries as sources of N₂O emission to the atmosphere: The estuary of the River Colne, Essex, UK. *Mar. Ecol. Prog. Ser.* **1998**, *164*, 59–71. [[CrossRef](#)]
20. Dong, L.F.; Nedwell, D.B.; Underwood, G.J.C.; Thornton, D.C.O.; Rusmana, I. Nitrous oxide formation in the Colne estuary, England: The central role of nitrite. *Appl. Environ. Microbiol.* **2002**, *68*, 1240–1249. [[CrossRef](#)] [[PubMed](#)]

21. Adams, C.A.; Andrews, J.E.; Jickells, T. Nitrous oxide and methane fluxes vs. carbon, nitrogen and phosphorous burial in new intertidal and saltmarsh sediments. *Sci. Total Environ.* **2012**, *434*, 240–251. [[CrossRef](#)] [[PubMed](#)]
22. Ferron, S.; Ortega, T.; Gomez-Parra, A.; Forja, J.M. Seasonal study of dissolved CH₄CO₂ and N₂O in a shallow tidal system of the bay of Cadiz (SW Spain). *J. Mar. Syst.* **2007**, *66*, 244–257. [[CrossRef](#)]
23. Magalhaes, C.M.; Wiebe, W.J.; Joye, S.B.; Bordalo, A.A. Inorganic nitrogen dynamics in intertidal rocky biofilms and sediments of the Douro River estuary (Portugal). *Estuaries* **2005**, *28*, 592–607. [[CrossRef](#)]
24. Young, C.; Tamborski, J.; Bokuniewicz, H. Embayment scale assessment of submarine groundwater discharge nutrient loading and associated land use. *Estuar. Coast. Shelf Sci.* **2015**, *158*, 20–30. [[CrossRef](#)]
25. Diaz, R.J.; Rosenberg, R. Spreading dead zones and consequences for marine ecosystems. *Science* **2008**, *321*, 926–929. [[CrossRef](#)] [[PubMed](#)]
26. Stackelberg, P. *Relation between Land Use and Quality of Shallow, Intermediate, and Deep Ground-Water in Nassau and Suffolk Counties, Long Island, New York*; U.S. Geological Survey: Reston, VA, USA, 1995.
27. Rapaglia, J.; Grant, C.; Bokuniewicz, H.; Pick, T.; Scholten, J. A GIS typology to locate sites of submarine groundwater discharge. *J. Environ. Radioact.* **2015**, *145*, 10–18. [[CrossRef](#)] [[PubMed](#)]
28. Young, C.; Kroeger, K.; Hanson, G. Limited denitrification in glacial deposit aquifers having thick unsaturated zones (Long Island, USA). *Hydrogeol. J.* **2013**, *21*, 1773–1786. [[CrossRef](#)]
29. Georgas, N. Tidal Hydrodynamics and Bedload Transport in a Shallow, Vegetated Harbor (Stony Brook Harbor, Long Island, New York): A Modeling Approach with Management Implications. In *Marine Environmental Science*; Stony Brook University: Stony Brook, NY, USA, 2001; p. 166.
30. Paulsen, R.J.; Smith, C.F.; O'Rourke, D.; Wong, T.F. Development and evaluation of an ultrasonic ground water seepage meter. *Ground Water* **2001**, *39*, 904–911. [[CrossRef](#)] [[PubMed](#)]
31. Durand, J.M. Characterization of the Spatial and Temporal Variations of Submarine Groundwater Discharge Using Electrical Resistivity and Seepage Measurements. In *Geosciences*; Stony Brook University: Stony Brook, NY, USA, 2014; p. 182.
32. Charette, M.A.; Allen, M.C. Precision ground water sampling in coastal aquifers using a direct-push, shielded-screen well-point system. *Ground Water Monit. Remediat.* **2006**, *26*, 87–93. [[CrossRef](#)]
33. Kana, T.M.; Darkangelo, C.; Hunt, M.D.; Oldham, J.B.; Bennett, G.E.; Cornwell, J.C. Membrane inlet mass-spectrometer for rapid high-precision determination of N₂, O₂ and Ar in environmental water samples. *Anal. Chem.* **1994**, *66*, 4166–4170. [[CrossRef](#)]
34. Weiss, R.F. The solubility of nitrogen, oxygen and argon in water and seawater. *Deep Sea Res. Oceanogr. Abstr.* **1970**, *17*, 721–735. [[CrossRef](#)]
35. Weiss, R.F.; Price, B.A. Nitrous-oxide solubility in water and seawater. *Mar. Chem.* **1980**, *8*, 347–359. [[CrossRef](#)]
36. Weymann, D.; Well, R.; Flessa, H.; von der Heide, C.; Deurer, M.; Meyer, K.; Konrad, C.; Walther, W. Groundwater N₂O emission factors of nitrate-contaminated aquifers as derived from denitrification progress and N₂O accumulation. *Biogeosciences* **2008**, *5*, 1215–1226. [[CrossRef](#)]
37. Walter, S.; Peeken, I.; Lochte, K.; Webb, A.; Bange, H.W. Nitrous oxide measurements during EIFEX, the European Iron Fertilization Experiment in the Subpolar South Atlantic Ocean. *Geophys. Res. Lett.* **2005**, *32*. [[CrossRef](#)]
38. Heaton, T.H.E.; Vogel, J.C. Excess air in groundwater. *J. Hydrol.* **1981**, *50*, 201–216. [[CrossRef](#)]
39. Holocher, J.; Peeters, F.; Aeschbach-Hertig, W.; Kinzelbach, W.; Kipfer, R. Kinetic model of gas bubble dissolution in groundwater and its implications for the dissolved gas composition. *Environ. Sci. Technol.* **2003**, *37*, 1337–1343. [[CrossRef](#)]
40. Aeschbach-Hertig, W.; Beyerle, U.; Kipfer, R. Excess air in groundwater as a proxy for paleo-humidity. *Geochim. Cosmochim. Acta* **2002**, *66*, A8–A8.
41. Robinson, C.; Li, L.; Barry, D.A. Effect of tidal forcing on a subterranean estuary. *Adv. Water Resour.* **2007**, *30*, 851–865. [[CrossRef](#)]
42. Xin, P.; Robinson, C.; Li, L.; Barry, D.A.; Bakhtyar, R. Effects of wave forcing on a subterranean estuary. *Water Resour. Res.* **2010**, *46*. [[CrossRef](#)]
43. Robinson, C.; Li, L.; Prommer, H. Tide-induced recirculation across the aquifer-ocean interface. *Water Resour. Res.* **2007**, *43*. [[CrossRef](#)]

44. Xin, P.; Wang, S.S.J.; Lu, C.; Robinson, C.; Li, L. Nonlinear interactions of waves and tides in a subterranean estuary. *Geophys. Res. Lett.* **2015**, *42*, 2277–2284. [[CrossRef](#)]
45. Pabich, W.J.; Valiela, I.; Hemond, H.F. Relationship between DOC concentration and vadose zone thickness and depth below water table in groundwater of Cape Cod, USA. *Biogeochemistry* **2001**, *55*, 247–268. [[CrossRef](#)]
46. Eckhardt, D.A.V.; Stackelberg, P.E. Relation of groundwater quality to land-use on long-island, New-York. *Ground Water* **1995**, *33*, 1019–1033. [[CrossRef](#)]
47. Moseman-Valtierra, S.; Gonzalez, R.; Kroeger, K.D.; Tang, J.; Chao, W.C.; Crusius, J.; Bratton, J.; Green, A.; Shelton, J. Short-term nitrogen additions can shift a coastal wetland from a sink to a source of N₂O. *Atmos. Environ.* **2011**, *45*, 4390–4397. [[CrossRef](#)]
48. Hartnett, H.E.; Seitzinger, S.P. High-resolution nitrogen gas profiles in sediment porewaters using a new membrane probe for membrane-inlet mass spectrometry. *Mar. Chem.* **2003**, *83*, 23–30. [[CrossRef](#)]
49. Singleton, M.J.; Esser, B.K.; Moran, J.E.; Hudson, G.B.; McNab, W.W.; Harter, T. Saturated zone denitrification: Potential for natural attenuation of nitrate contamination in shallow groundwater under dairy operations. *Environ. Sci. Technol.* **2007**, *41*, 759–765. [[CrossRef](#)] [[PubMed](#)]
50. Laverman, A.M.; Garnier, J.A.; Mounier, E.M.; Roose-Amsaleg, C.L. Nitrous oxide production kinetics during nitrate reduction in river sediments. *Water Res.* **2010**, *44*, 1753–1764. [[CrossRef](#)] [[PubMed](#)]
51. LaMontagne, M.G.; Duran, R.; Valiela, I. Nitrous oxide sources and sinks in coastal aquifers and coupled estuarine receiving waters. *Sci. Total Environ.* **2003**, *309*, 139–149. [[CrossRef](#)]
52. Martin, J.B.; Cable, J.E.; Smith, C.; Roy, M.; Cherrier, J. Magnitudes of submarine groundwater discharge from marine and terrestrial sources: Indian River Lagoon, Florida. *Water Resour. Res.* **2007**, *43*. [[CrossRef](#)]
53. Deurer, M.; von der Heide, C.; Bottcher, J.; Duijnisveld, W.H.M.; Weymann, D.; Well, R. The dynamics of N₂O near the groundwater table and the transfer of N₂O into the unsaturated zone: A case study from a sandy aquifer in Germany. *Catena* **2008**, *72*, 362–373. [[CrossRef](#)]
54. Minamikawa, K.; Wagai, R.; Nishimura, S.; Yagi, K. Heterotrophic denitrification constrains the upper limit of dissolved N₂O-nitrate concentration ratio in agricultural groundwater. *Nutri. Cycl. Agroecosyst.* **2015**, *101*, 181–191. [[CrossRef](#)]
55. Burnett, W.C.; Bokuniewicz, H.; Huettel, M.; Moore, W.S.; Taniguchi, M. Groundwater and pore water inputs to the coastal zone. *Biogeochemistry* **2003**, *66*, 3–33. [[CrossRef](#)]
56. Weymann, D.; Well, R.; von der Heide, C.; Bottcher, J.; Flessa, H.; Duijnisveld, W.H. Recovery of groundwater N₂O at the soil surface and its contribution to total N₂O emissions. *Nutri. Cycl. Agroecosyst.* **2009**, *85*, 299–312. [[CrossRef](#)]
57. Vilain, G.; Garnier, J.; Tallec, G.; Tournebize, J. Indirect N₂O emissions from shallow groundwater in an agricultural catchment (Seine Basin, France). *Biogeochemistry* **2012**, *111*, 253–271. [[CrossRef](#)]

